

# Experimental study of nanofluid effects on heat transfer in closed cycle system in shell and tube heat exchangers at Isfahan power plant

## Authors

Ali Reza Yousefnejad<sup>a</sup>  
 Mohammad Mahdi Heyhat<sup>b\*</sup>  
 Amir Homayoun Meghdadi<sup>a</sup>

<sup>a</sup> Department of Mechanical Engineering, Najafabad Branch, Islamic Azad University, Najafabad, Iran

<sup>b</sup> Faculty of Mechanical Engineering, Tarbiat Modares University, Tehran, Iran

## ABSTRACT

*The present study investigated the effect of distilled-water/ silver nanofluid on heat transfer in a closed cooling system of one of the electrical energy generation units at Isfahan power plant. The difference between this study and previous researches refers to silver properties which have a high thermal conductivity and is non-toxic, hydrophilic and eco-friendly. Distilled water/ silver nanofluid with 20 nm average diameter and 0.1% volume fraction was purchased from Iranian nanomaterials' Pishgaman company. The volume fractions 0.01%, 0.025%, 0.05%, 0.075% were prepared in the laboratory and thermophysical properties were practically measured in the laboratory. Nanofluids with flow rates from 0.14 to 0.26 kg/s and volume fraction from 0.01% to 0.1% passed through the tubes of heat exchanger and were evaluated in the Reynolds number range of 1500 to 4000. This study was aimed to achieve the overall heat transfer coefficients and pressure drop of the system. According to the system performance index, the results showed that nanofluid can be used to increase the efficiency of heat exchangers and, as an appropriate method, to reduce the dimensions of the exchangers. The results showed that nanofluid increased heat transfer coefficient by 16%. Pressure drop of nanofluid, however, have no significant change compared with the pressure drop of pure water.*

## Article history:

Received : 13 December 2015  
 Accepted : 21 February 2016

**Keywords:** Closed System, Heat Transfer Coefficient, Nanofluid, Shell and Tube Heat Exchanger, Silver Nanoparticles.

## 1. Introduction

Heat exchangers are devices that are used for heat transfer between different fluids. This equipment is widely used in various industries such as cooling and heating, chemical processes, ventilation, power plants as well as cooling the electronic components. One of the most common types of heat exchangers used in the industry is shell and tube heat

exchanger, known in this study as closed cycle cooling system. These heat exchangers are commonly used to transfer heat between two fluids. The components of a shell and tube heat exchanger include tube, tube sheet, shell, front head, back head and baffles. This type of heat exchanger has many tubes containing fluid whose external part is in contact with another fluid and heat transfer is made possible through the interface, i.e. the body or wall of the tube. The material of tubes should be selected in such a way that in

\*Corresponding author: Mohammad Mahdi Heyhat  
 Address: Faculty of Mechanical Engineering, Tarbiat Modares University, Tehran, Iran  
 E-mail address: mmheyhat@modares.ac.ir

addition to endurance is a good conductor of heat.

The blades, baffles and other existing technologies are used to increase heat transfer, but these methods cannot meet the high heat transfer in different industries and, nevertheless, increase the pressure drop. Therefore, it is essential to find better ways to increase heat transfer. Fluids such as water, Ethylene glycol, oils, etc. play a vital role in the process of heat transfer in industry. However, these fluids generally have poor heat transfer characteristics compared to the most solids and cause many problems in the design of heat exchangers and their compacting. Recent advances in suspending ultra-fine particles of solids in fluids, have been proposed as a new approach in heat transfer operations. Various types of solid particles, including metal particles and metal oxides are added to the fluid to form a suspension to improve its thermal performance.

Closed cycle cooling system is a system in which distilled water is circulating inside the tubes in a closed cycle and is not evaporated due to lack of exposure to air, so there is not much change in its composition. Similar to any water network, the closed cycle system needs to upgrade hydro-chemical waste, but because it has a low loss, the sanitation cost in good conditions of the system is not much. For the system to work well, the raw water and make-up water must be in good quality. Water speed in closed cycle system is generally low, between 0.3 and 3.1 meters per second. The temperature difference created in this system varies from 6 to 10 degrees Celsius. The closed cycle system needs very little make-up water if there are no leaks in pumps and consumption centers. The system is equipped with an expansion tank and an outlet valve for partial evaporation. Although makeup water is distilled water and the risk of sediment and erosion is low, it is required to test the water within a definite period of time and compare the amount of water-soluble materials with the feed water tank. As there are often different alloys and metals in the direction of moving fluid, there is a possible risk of galvanic corrosion. Since the makeup water contains a small amount of oxygen, corrosion by oxygen is low.

Application of nanofluids to improve heat transfer has attracted many researchers. Farajollahi et al. [1] evaluated the heat transfer properties of water/ aluminum oxide and water/ titanium oxide nanofluids under

turbulent flow conditions in a shell and tube heat exchanger, with volume fraction ranges of 0.3% -2% and 0.15% - 0.75% and Peclet number between 20000 and 60000. Their results showed that the heat transfer properties of nanofluids were significantly improved with an increase in Peclet number. Nanoparticles added to the base fluid improved heat transfer performance and greater heat transfer coefficient was observed in a constant Peclet number. The results of testing water/ aluminum oxide nanofluid in a fixed condition showed that volume fractions 0.3% and 0.75% increased 21% and 23%, respectively. Seifi [2] calculated heat transfer coefficient of water/ aluminum oxide in the finned tube heat exchanger at different concentrations and reported 45% increase of heat transfer coefficient of nanofluids in the volume fraction of 1% compared to the base fluid. Peyghambarzadeh et al. [3] experimentally evaluated the forced convective heat transfer of water/ aluminum oxide nanofluid in car radiators under turbulent flow. The experimental system used in this study consisted of flow lines, a storage tank, heater, centrifugal pump, flow meter, blower fan and cross-flow heat exchanger. The total volume of fluid in circulation was constant in all experiments. An electrical heater was used for heating the fluid and a controller to maintain the temperature between 40 and 80°C. Five different concentrations of nanofluid in the range of 0.01-0.1% by volume were prepared by adding aluminum oxide nanoparticles into the water. The experimental results showed that increasing the flow rate of the fluid could improve the heat transfer performance, while inlet fluid temperature into the radiator had little effect. Meanwhile, the use of nanofluids with low concentration could increase heat transfer efficiency up to 45% compared with pure water lift.

Zamzamin et al. [4] analyzed forced convective heat transfer coefficient in turbulent flow in a two-tube heat exchanger and a plate with alumina oxide nanoparticles in ethylene glycol. The results showed that the nanoparticles in the base fluid caused a significant increase in the forced convective heat transfer coefficient of the base fluid. The largest and smallest increase rates in the tests were reported to be 49% and 3%, respectively.

Gadson et al. [5] experimentally investigated the heat transfer coefficient of water/ silver nanofluid in a heat exchanger

tube with an internal diameter of 4.3 mm as a non-parallel flow in heat transfer laboratory. Their results indicated that the nanoparticles substantially increased the heat transfer performance of base fluid, water, under the same Reynolds number. A 0.9% volume increase of silver particles in water increased the heat transfer coefficient by 69.3%.

Samchandra et al. [6] conducted a study using water/ aluminum oxide nanofluid with average particle diameters of 20,40,60,80 nm and volume concentration of 0.012 in the laminar flow regime. The results revealed that the thermal conductivity of the fluid increased as the diameter of the nanoparticles was reduced, followed by an increase in heat transfer coefficient. The major drawback of nanofluid is that the coefficient of friction is also increased. The particles (20 nm) had the maximum heat transfer and coefficient of friction among all the particles used. Arvind Deharan [7] experimentally investigated the heat transfer properties of water/ aluminum nitride nanofluid in a shell and tube heat exchanger, because of its high melting point, low density and high structural stability, developed from the synthesis of aluminum nitride nanoparticles with water. The heat transfer properties of these nanofluids, such as thermal conductivity and heat transfer coefficient were investigated. The results showed that this nanofluid had a higher thermal transfer characteristics and 9.68% more efficiency than water. It has also been proven experimentally that this nanofluid has the potential to be used as an advanced heat transfer fluid.

In another study, Amani et al. [8] evaluated the effect of the volume fraction effect of nanoparticles in water/ titanium oxide nanofluid on the properties of heat transfer and pressure drop in a wide range of nanoparticles volume fraction and Reynolds number in a turbulent flow. It is seen that by increasing the Reynolds number or volume fraction of particles, heat transfer and pressure drop are increased. In addition, all nanofluids, compared to distilled water, had a higher heat transfer and pressure drop. The heat transfer rate of nanofluid with concentration of 0.002 was higher than that of the base fluid, while both of them had the same pressure drop in the low Reynolds numbers. Nanofluid with concentrations of 0.01 and 0.02 showed a significant increase in both heat transfer and pressure drop. Therefore, dilute nanofluid is recommended to be used in low Reynolds number.

In an experimental study, Gadson et al. [9]

investigated the heat transfer of water/ silver nanofluid in a counter flow shell and tube heat exchanger. The findings indicated that the percentage increase of heat transfer in volume fractions 0.01%, 0.03% and 0.01% were reported to be 9.2%, 10.87% and 12.4%, respectively. Further, an increase in the volume fraction of the silver particles enhanced the heat transfer coefficient and efficiency of water/ silver nanofluid. Maximum increase was recorded in the heat transfer coefficient of 12.4% and efficiency of 6.14%. It was also shown that the significant increase in the coefficient of heat transfer was due to increased thermo-physical properties of nanofluids, and delays in the development of the boundary layer in the entrance areas were due to the rise the nanoparticles. Finally, increased pressure drop of water/ silver nanofluid was reported to be 0.04% at Reynolds number 25000 compared to the pure water.

Afshoon et al. [10] compared the heat transfer rate and friction coefficient of water/ copper oxide nanofluid with water, as a base fluid, in an incompressible, homogeneous and turbulent flow in a shell and tube heat exchanger using the numerical methods of Fluent software. Given the constant thermo-physical properties of nanofluid in nano-sized particles at volume fraction of 0.015, 0.031, 0.078, 0.157 and 0.236% in the range of 6000-31000 Reynolds number as a fully developed turbulent flow in comparison with the base fluid, water, and by setting the initial conditions and boundary conditions based on temperature and nanofluids input speed, the heat transfer coefficient, overall heat transfer coefficient and pressure drop were increased with a rise in volume fraction and nanofluid Reynolds number. The results showed the improved thermal conductivity to be 32% compared to water base fluid.

According to the studies, the experimental study of the effect of an eco-friendly nanofluid in a closed cooling system of a power plant will be of considerable value. Hence, a similar closed to that of Isfahan power plant was built in this study, and in the actual operation of the plant, the behavior of heat transfer and pressure drop of distilled water/ silver nanofluid in a closed cycle cooling system, a type of shell and tube heat exchanger, was studied for a range of particle volume fraction of 0.01-0.1% and flow rate of 0.14-0.26 kg/s. Pure silver, whose physical and thermal properties are presented in Table 1, had a high electrical and thermal conductivity, and is able to eliminate different

pathogenic microorganisms. In this study, the main reasons for the use of silver nanoparticles are the non-toxicity, eco-friendliness, hydrophilicity, good thermal properties even at low concentrations and insensitivity to the body.

The X-ray of silver nanoparticles is show in Fig. 1. An image of the nanostructure after production of water/ silver nanofluid is shown in Fig. 2, demonstrating the dispersion of particles in the fluid.

**Nomenclature**

- P* Pressure (kg/cm<sup>2</sup>)
- Nu* Nusselt number
- Re* Reynolds number
- Pr* Prandtl number
- St* Stanton number

- $\dot{m}$  Mass flow (kg/s)
- $C_p$  Specific Heat (J/kg°C)
- $h_i$  Heat transfer coefficient (W/m<sup>2</sup>K)
- $u_i$  Speed (m/s)
- $k$  Thermal conductivity (W/mK)

**Greek symptoms**

- $\rho$  Density (kg/m<sup>3</sup>)
- $\mu$  Dynamic viscosity (kg/ms)
- $\phi_V$  Volume ratio of particles
- $\Delta T_{lm}$  Logarithmic mean temperature difference
- $\rho$  Density (kg/m<sup>3</sup>)

**Subtitles**

- f* Base fluid
- nf* Nanofluid
- p* Nanoparticles

**Table1.** Physical and thermal properties of silver nanofluid

Mean diameter nm	Density Kg/cm <sup>3</sup>	Specific heat J/kg°C	Thermal conductivity W/m°C	Nanoparticle
20	10490	232	429	Silver

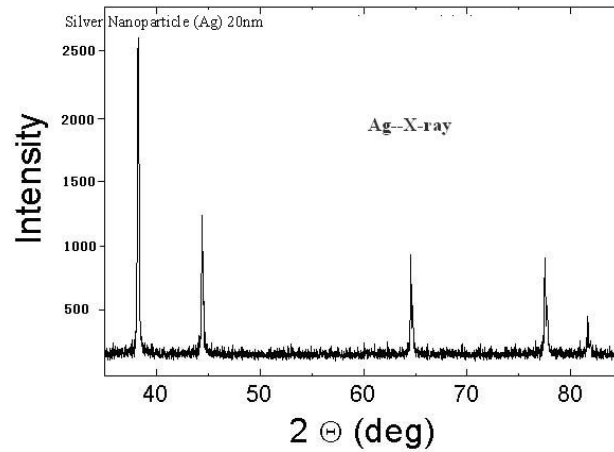


**Fig. 1.** X-ray of silver nanoparticles of 20 nm in diameter

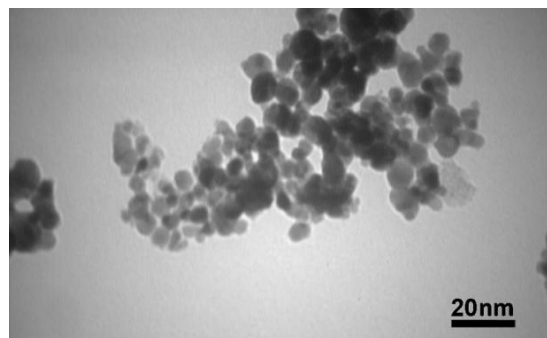


**Fig. 2.** Nanostructure after production of distilled-water/silver nanofluid

## 2. Laboratory system and test method

The overview of the test device is shown in Fig. 3. Generally, the system includes two current loops (nanofluids and hot water), two shell and tube heat exchangers made of copper (nanofluid passes through pipes and hot water through the membrane), the cooling system of nanofluid (radiator and fan blower), 20-liter nanofluid storage tank, 25-liter tank, and electric heater to heat the water, bypass pipe, four thermometers (R.T.D) to measure the fluid temperature at the input and output transducers, temperature controller, four flowmeters, four barometers, a differential pressure meter and two stainless steel centrifugal pumps to provide the necessary flow rate.

The test system is shown in Fig. 4, including shell and tube exchanger which is shown schematically in Fig. 5, installed on the chassis. The heat exchanger, HCF heat exchanger based on TEMA standard, has two

tube passes and one shell pass. Nanofluid passes through 28 tubes with an outer diameter of 25.6 mm and length of 354 mm. Hot water passes through the shell with an inner diameter of 78 mm. The tube step is 8 mm in which 25% baffles with 43.75 mm distance from each other are used. Heat exchanger and pipe fittings are insulated to prevent heat exchange with the environment. The flow rate is controlled by two globular valves, one in the main line of flow and another in the bypass line. The water and nanofluid flowmeters have been collected by weighing the water and nanofluid and calibrated in a certain period. Four thermometers are installed at the input and output of the tubes connected to the heat exchanger. Thermometers are calibrated using the reference thermocouple, type PT100. Measurement error of fluid temperature calculated by thermometers type R.T.D is  $\pm 1^\circ\text{C}$ . Barometers are of Wicca Glycerin type in the interval 0-60 psi and have been

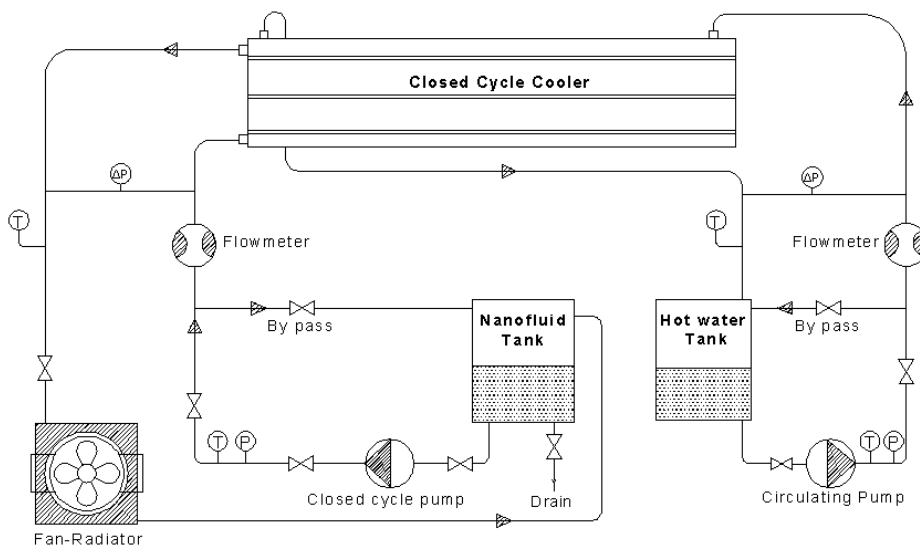


Fig. 3. Experimental closed cycle system



Fig. 4. Closed cycle system built for testing

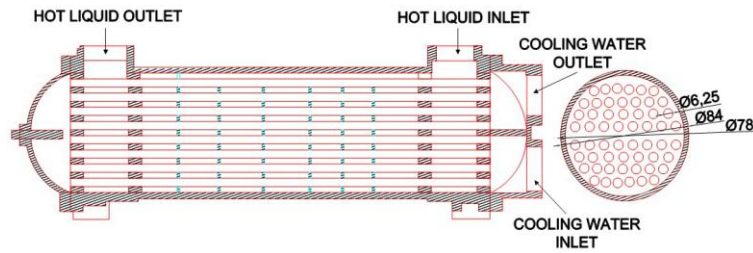


Fig. 5. Schematic of shell and tube heat exchanger with a shell pass and two tube passes

calibrated in the calibration laboratory by reference devices and are installed at the inputs and outputs of the shell and tubes of the heat exchanger. Data are collected visually and the barometer error is 0.1. However, to read the pressure difference, the differential pressure meter FaxPro 0-2 psi, with 0.1 psi error, is used.

Tubes are straight and not U-shaped. The fluid in the pipe inlet and outlet on passes through one side of exchanger and on the shell side passes through both sides of the shell. Distilled water/ silver nanofluid flows from the pipes and the hot fluid passes through the exchanger shell. A 1-kw heater is installed inside the hot water tank, which keeps the inlet fluid temperature of the shell constant via a controller. At first, the source water heater is turned on and both pumps are placed in the service to initiate fluid flow in order to make the system stable at the same time. Data collection is done after the conditions are stable. Each test is repeated several times under its particular conditions to reduce the error. The test is performed at various fixed temperatures at shell inlet of exchanger and different flow rates of nanofluid with different volume fractions.

In this study, distilled water/ silver nanofluid with volume fractions of 0.01%, 0.025%, 0.05% and 0.075% and 0.1% silver particles were used to study the effect of nanofluid on improving the heat transfer in a shell and tube heat exchanger. Distilled-water/ silver nanofluid was provided through a two-step method. In the two-step method, prepared nano-powder was stabilized in the base fluid by ultrasonic method. The silver nano-powder with mean diameter of 20 nm was stabilized by ultrasonic device with a certain power in the distilled-water base fluid for 3 hours. Notably, any additional material or stabilizer was not added to the nanofluid. An electromagnetic homogenization device and ultrasonic bath was used to stabilize the nanofluid. The produced nanofluid was kept in a glass container in closed environment about 6 months so that no sediment of nanofluid was observed on the bottom of the container.

### 3. Nanofluid and its specifications

The dynamic viscosity of distilled-water/ silver nanofluid was measured in the laboratory by Brookfield digital viscometer (DV II Pro) and thermal conductivity of distilled-water/ silver nanofluid was determined by Hawks flux conductometer at temperatures 40, 50 and 65°C with volume fractions 0.01%, 0.025%, 0.05%, 0.075% and 0.1%. Specific heat and density of the nanofluid was practically measured in the laboratory. Specific heat capacity was achieved by differential calorimetric analysis. The temperature of both sample and the reference materials was increased with the same rate and the specific heat of the sample required to raise the temperature was calculated by measuring the difference in temperature. The uncertainty of measurement was approximately 3%. The nanofluid density of the fluid had been measured by the manufacturer, but it was measured again in Isfahan power plant by Anton Paar-DMA5000 machine with different volume fractions. It is one of the most common types of digital densitometers. The device has a U-shaped cell with volume. The DMA 5000 device was calibrated by pure water and air with an uncertainty of  $\pm 0.00015 \text{ gr/cm}^3$  to test different compounds. If the cell is cleaned well and the device is carefully calibrated, the repeatability of device for compounds with specific damping (including compounds with viscosity close to water) can be expected to reach the uncertainty level of  $\pm 0.00003 \text{ gr/cm}^3$ . Because the most power plant equipment operates in real conditions at a temperature about 50°C, only the properties of nanofluid at 50°C are shown in Table 2.

### 4. Formulations and data analysis methods

The primary experiments were done with the base fluid, distilled water to gain some experience in working with the device and base the testing and calculation with distilled-water/ silver nanofluid. Then, the experiments with distilled- water/ silver nanofluid in

**Table 2.** Properties of distilled-water/silver nanofluid at 50°C

Volume Fraction %	Density Kg/cm <sup>3</sup>	Specific Heat J/kg°C	Thermal Conductivity W/m°C	Viscosity Kg/ms
0.1	1086.46	3793.67	0.654	0.00076
0.075	1062.57	3882.35	0.59	0.00073
0.05	1039.16	3975.19	0.654	0.0007
0.025	1015.63	4071.27	0.648	0.00068
0.01	1002.06	4132.75	0.644	0.00067
Dis-water	986.30	4177.00	0.643	0.00059

different volume fractions were repeated at the same temperatures and flow rates used for distilled-water. Distilled-water was used as cold fluid in the tubes and hot fluid in the shell. After a stable state was achieved, the temperatures at the inputs and outputs were measured. When the temperature showed a constant value for about 20 minutes, it was found out that it reached its steady state. The heat transfer rate of distilled-water/ distilled-water is shown in Fig. 6.

$$Q = \dot{m}_c C_{p,c} (T_{out,c} - T_{in,c}) \quad (1)$$

$$= \dot{m}_h C_{p,h} (T_{out,h} - T_{in,h})$$

The heat transfer from the hot fluid to cold fluid is calculated using the following equation, where  $\dot{m}_c$  and  $\dot{m}_h$  represent the mass flow rate of distilled-water in the tube side and shell side, respectively.  $T_{out}$  and  $T_{in}$  show the input and output temperature in both sides of the converter, respectively. With a cross section of all the tubes, the total heat transfer coefficient,  $U$ , is obtained as follows:

$$Q = U_i A_i \Delta T_{lm} \quad (2)$$

Overall heat transfer coefficient,  $U$ , is obtained by the above equation where  $\Delta T_{lm}$  indicates logarithmic mean temperature difference that is defined for a Counter flow in a heat exchanger with two tube passes and one shell pass [11]:

$$\Delta T_{lm} = \frac{\Delta T_1 - \Delta T_2}{\ln\left(\frac{\Delta T_1}{\Delta T_2}\right)} \quad (3)$$

$$\Delta T_{lm,PF} \rightarrow \begin{cases} \Delta T_1 = T_{h,i} - T_{c,i} \\ \Delta T_2 = T_{h,o} - T_{c,o} \end{cases} \quad (4)$$

The heat transfer coefficient of the flow within the pipe in steady state is usually expressed by the following equation [11]:

$$(h_i d_i) / k_f = j_h Re Pr^{0.33} \left(\frac{\mu}{\mu_w}\right)^{0.14} \quad (5)$$

where  $j_h$  is heat transfer factor. This factor is similar to the coefficient of friction in the relations used to determine the pressure drop. Heat transfer factor is defined as follows [11]:

$$j_h = St Pr^{0.67} \left(\frac{\mu}{\mu_w}\right)^{-0.14} \quad (6)$$

$$St = \frac{Nu}{Re Pr} = \frac{h_i}{\rho u_i C_p} \quad (7)$$

Also, to calculate the heat transfer coefficient of warm fluid on the outer surface of the inner tube (the shell), the following equation was used to obtain  $h_o$ :

$$(h_o d_e) / k_f = j_h Re Pr^{0.33} \left(\frac{\mu}{\mu_w}\right)^{0.14} \quad (8)$$

$d_e$ , shell diameter (hydraulic diameter) for the triangular arrangement of the relationship is calculated as follows:

$$d_e = \frac{1.1}{d_o} (P_t^2 - 0.917 d_o^2) \quad (9)$$

With a heat transfer coefficient of liquid inside the tube and the liquid on the outer surface of the pipe,  $U$ , the overall heat transfer coefficient is obtained using the following equation:

$$\frac{1}{U} = \frac{1}{h_i} + \frac{1}{h_o} \quad (10)$$

The heat transfer rate of distilled-water/ distilled-water is obtained by the above equations (Fig. 6). Figure 6 shows that by increasing the flow of water passing through the tubes, heat transfer rate is also increased.

Comparison of the overall heat transfer coefficient measured and predicted values from the equation 10 for distilled-water/ distilled-water is shown in Fig. 7. As shown,

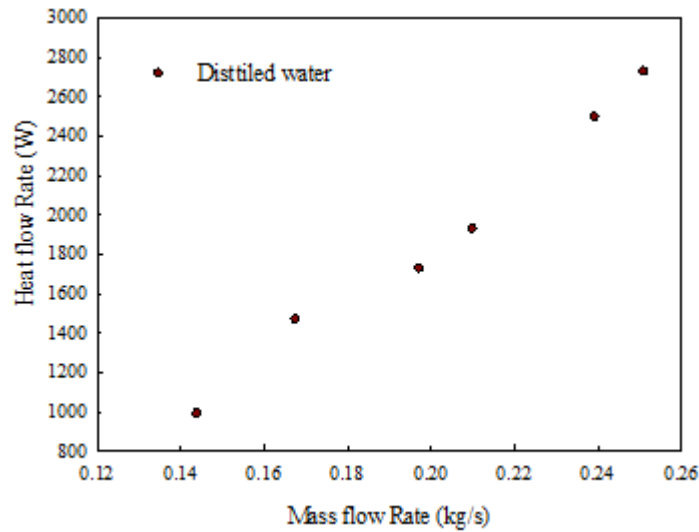


Fig. 6. The heat transfer rate of distilled-water/distilled-water

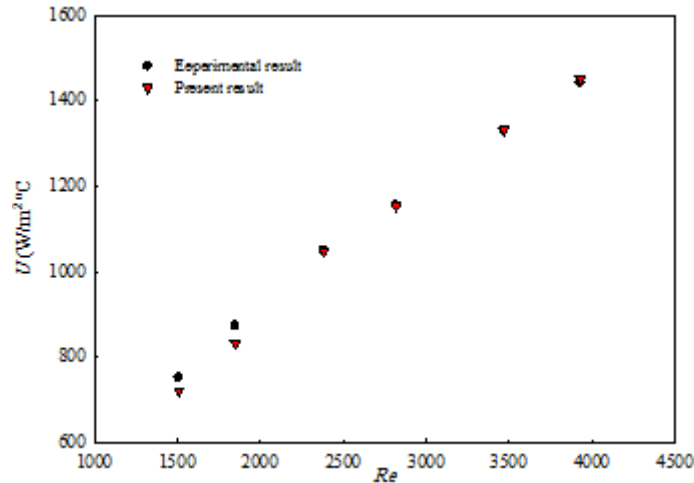


Fig. 7. Comparison between the measured overall heat transfer coefficient and simulated values using distilled-water

there is a good agreement between the measured and simulated values. The minimum difference was 0.12% and the maximum difference was 4.6% with an average of 2.4%. Differences seen in Fig. 7 may be due to measurement errors. In this test, high accuracy was applied to minimize measurement error.

After experimenting with distilled-water and achieving heat transfer coefficients and overall heat transfer coefficient, the experiment was repeated with the distilled-water/ silver nanofluid flowing in the tube side.

The heat exchange between the nanofluid inside the tube and shell side fluid is calculated as follows:

$$Q_{nf} = \dot{m}_{nf} C_{p,nf} (T_{out} - T_{in})_{nf} \quad (11)$$

where  $T_{out}$  represents average temperature of

output nanofluid,  $T_{in}$  average temperature of input nanofluid,  $C_{p,nf}$  nanofluid specific heat and  $\dot{m}_{nf}$  mass flow rate. The shell side fluid has not changed and the shell and tube diameters are fixed at this stage; the only thing that has changed is the nanofluid heat transfer coefficient inside the tubes. With the thermo-physical properties of distilled-water/ silver nanofluid in Table 1, we can obtain the heat transfer coefficient and the total heat transfer coefficient and compare the resulting changes with the results of distilled-water. Also, the Nusselt number for distilled-water/ silver nanofluid can be obtained by the same method and compared with the results of distilled-water.

## 5. Error Analysis

Measurement error is defined as the

between the actual value and the measured value. Error in each experiment depends on doing the test and the error of the equipment used in it. Depending on whether the error is fixed or changed in various tests, the sources of error can be divided into two categories, random errors and fixed errors.

If  $Z$  is a parameter obtained from two variables  $A$  and  $B$ , it is expressed as [12, 13]:

$$Z=A+B \tag{12}$$

The error  $\Delta Z$  is expressed as follows:

$$\Delta Z = \sqrt{(\Delta A)^2 + (\Delta B)^2} \tag{13}$$

Then, assume that two variables  $A$  and  $B$  are measured, thus  $Z =F (A, B)$ . If the  $A$  and  $B$  errors are  $\Delta A$  and  $\Delta B$ , respectively,  $\Delta Z$  is obtained as follows.

$$\Delta Z = \sqrt{\left(\frac{\partial F}{\partial A}\right)^2 \Delta A^2 + \left(\frac{\partial F}{\partial B}\right)^2 \Delta B^2} \tag{14}$$

Before the error measurement of calculated quantities such as heat transfer coefficient, Nusselt number, friction coefficient, the precision of measurement instruments and errors of the measured values need to be specified. The error of each of measured values is shown in Table 3.

Using the above equations and replacing the error of each of the measured values in Table 3, the values of maximum relative error calculated on the basis of the tests are given in Table 4.

### 6. Results and Discussion

Figure 8 compares the experimental data with the predicted values of Nusselt number against Reynolds number for distilled-water/silver nanofluid, with 0.1% volume fraction, where nanofluid moves through the pipes and the hot water passes through the shell.

**Table 3.** Errors in each of the measured values

Measuring Error	Symbol	Variable
±0/05mm	$U_D$	Tube diameter
±0.5 mm	$U_L$	Tube length
± 0.1°C	$U_{T_w}, U_{T_{bi}}, U_{T_{bo}}$	Temperature
±5cc	$U_V$	Decanter volume
±0.1s	$U_t$	Time
±0.05	$U_{k/k}$	Thermal Conductivity
±0.01	$U_{\mu/\mu}$	Dynamic Viscosity
±0.02	$U_{c_p/c_p}$	Specific heat capacity
±0.01	$U_{\rho/\rho}$	Density
±0.05	$U_{\Delta p/\Delta p}$	Pressure drop
±0/05mm	$U_D$	Tube diameter

**Table 4.** Maximum calculated relative error

Max Error value	Quantity
± 3.02%	Mean heat convection coefficient
± 5.92%	Mean Nusselt number
± 6.75%	Friction Factor

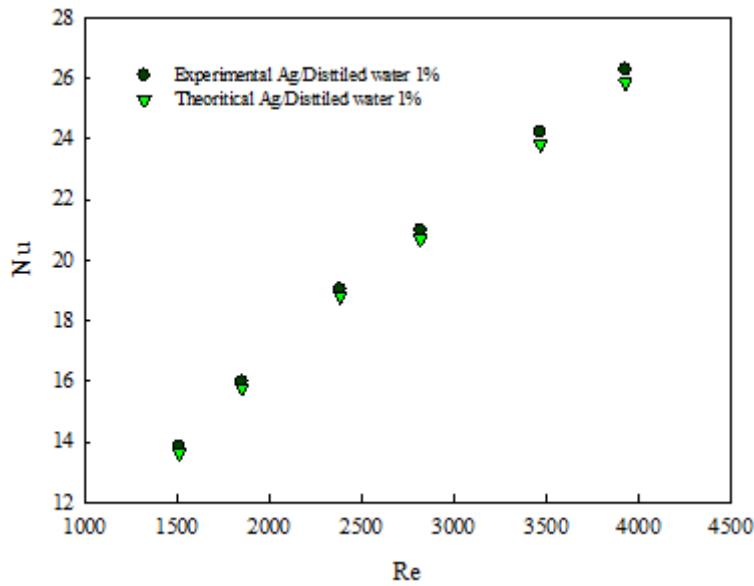


**Fig. 8.** Comparison of experimental and calculated values of Nusselt number against Reynolds number for distilled-water/silver nanofluid with a volume fraction of 0.1%

The heat transfer rate in terms of mass flow rate for pure water and nanofluid is shown in Fig. 9. The addition of nanoparticles even at very low volume fractions (0.01%) improved the heat flow rate. For example, in nanofluid mass flow rate of 0.19 kg/s, the heat transfer rate increased to 3.8%. In this experiment, distilled-water flow rate in the shell was 0.15 kg/s. Since the heat transfer coefficient is directly related to the fluid velocity, the increased fluid velocity increased the collisions between molecules; so, by increasing the mass flow rate, the heat transfer rate was increased. The presence of nanoparticles in pure water increased the heat

transfer and flow rates, so that the distance between the two curves of pure water and nanofluid was increased, thereby increasing the impact of nanofluid.

The heat transfer coefficient between distilled-water and nanofluid with volume fractions of 0.01%, 0.025%, 0.05% and 0.075% and 0.1% particles at different temperatures is shown in Fig. 10. As indicated, assuming a constant flow rate of 0.14 kg/s on the shell side and a constant flow rate of 0.21 kg/s in the tube side, the heat transfer coefficient is increased by increasing the temperature and number of the particles.

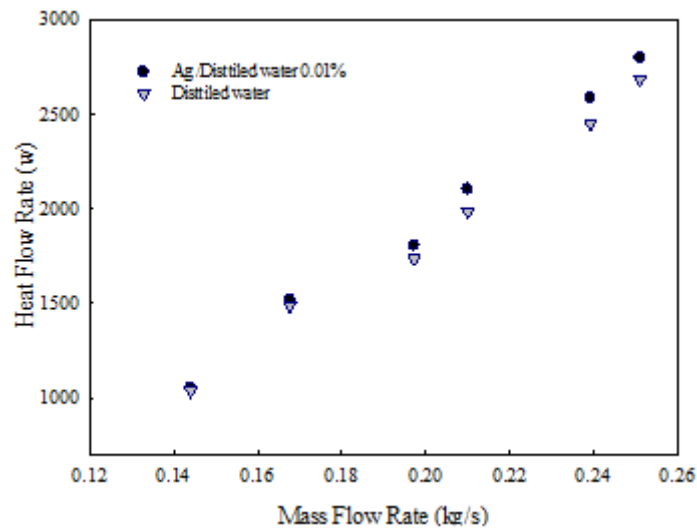


**Fig. 9.** Comparison of the heat transfer rate between the distilled-water and distilled-water/silver nanofluid with volume fraction of 0.01% at different flow rates

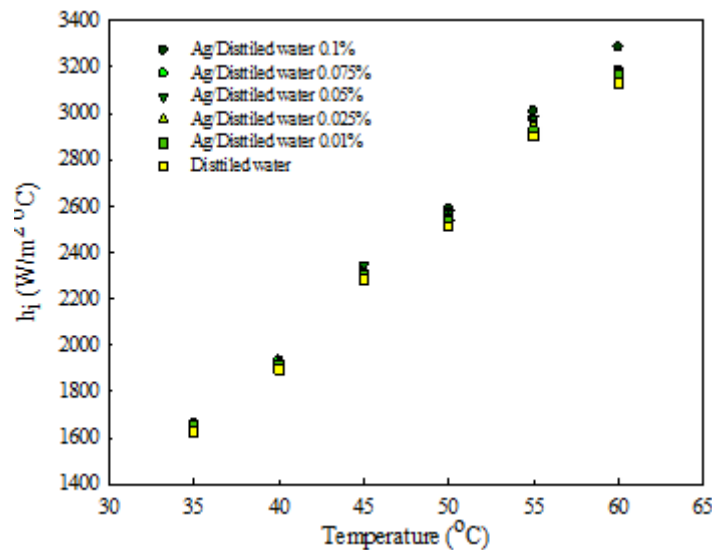


Fig. 10. The heat transfer coefficient of distilled- water/silver nanofluid with volume fractions 0.01%, 0.025%, 0.05%, 0.075% and 0.1% compared to the temperature in constant Reynolds number

The mobility and Brownian motion of the nanoparticles at higher temperatures can lead to increase fluid turbulence and further increase in the heat transfer coefficient. The minimum increase of the heat transfer of nanofluid compared with distilled water at the lowest temperature was 1.8% and maximum heat transfer at the highest temperature was 4.6%. Also, by increasing the volume fraction of silver nanoparticles at the constant flow rate, due to increasing the collision of particles, the heat transfer coefficient was increased. In a constant temperature and flow rate, increasing the volume fraction of the particles caused a rise in the heat transfer coefficient. This increase of the heat transfer coefficient can be linked to the intensified turbulence in the base fluid due to the presence of nanoparticles.

The overall heat transfer coefficient of distilled-water/ silver nanofluid compared to the Reynolds number for different volume fractions of particles is shown in Fig. 11. As shown, the overall heat transfer coefficient in constant Reynolds number is increased with a rise in the volume fraction of particles compared to the base fluid. Maximum increase in overall heat transfer coefficient of distilled-water/ silver nanofluid occurred in the volume fraction of 0.1%. In this state, as the Reynolds number increased up to 3900, the improvement in overall heat transfer coefficient was about 12.5%. At this level of Reynolds number, the increase of the overall heat transfer coefficients in volume fractions of 0.075%, 0.05%, 0.025% and 0.1% were 8.8%, 6.4%, 3.5% and 1.4%, respectively.

Figure 12 shows the increase ratio of the overall heat transfer of nanofluid in volume fractions of 0.01%, 0.025%, 0.05%, 0.075% and 0.1% compared to distilled water. As can be seen, the overall heat transfer coefficient of distilled-water/ silver nanofluid in all volume fractions has been increased compared to distilled-water.

The changes of Nusselt number versus Reynolds number at different temperatures with the volume fractions 0.01%, 0.075% and 0.05% are illustrated in Fig. 13. According to the results, the heat transfer rate of nanofluid in all volume fractions is higher than the base fluid and the amount of energy absorbed by the nanofluid is more than that of distilled-water.

The pressure drop during the distilled-water test was measured by installing a pressure drop gauge on the input and output pipes of the heat exchanger at different flows and temperatures. Then, the pressure drop was measured and recorded at the same flows and temperatures of nanofluid in various volume fractions. The comparison of the pressure drop of distilled-water and silver nanofluid with volume fractions of 0.01%, 0.025%, 0.05%, 0.075% and 0.1% is shown in Fig. 14, indicating the increase of pressure drop with a rise in the flow rate and volume fraction of particles.

Figure 15 indicates the pressure drop ratio of distilled-water/ silver nanofluid to that of distilled-water in the volume fractions of 0.01%, 0.025%, 0.05%, 0.075% and 0.1%. As shown, at constant temperatures and flow rates, the pressure drop in all volume fractions is more than that of distilled-water.

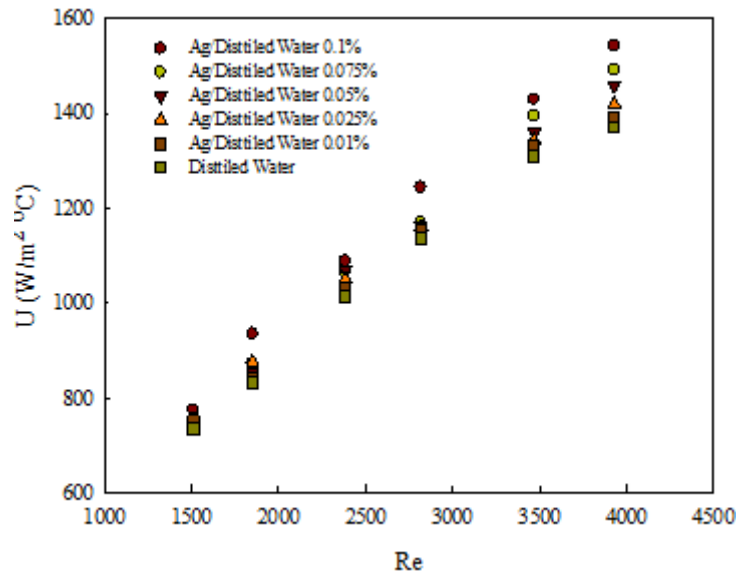


Fig. 11. Overall heat transfer coefficient of distilled-water/silver nanofluid compared to Reynolds number for different volume fractions of particles

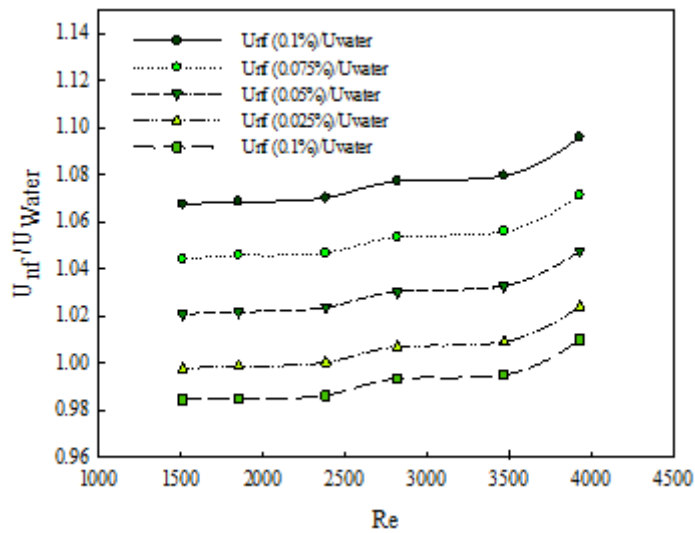


Fig. 12. Increase ratio of overall heat transfer of nanofluid and distilled water

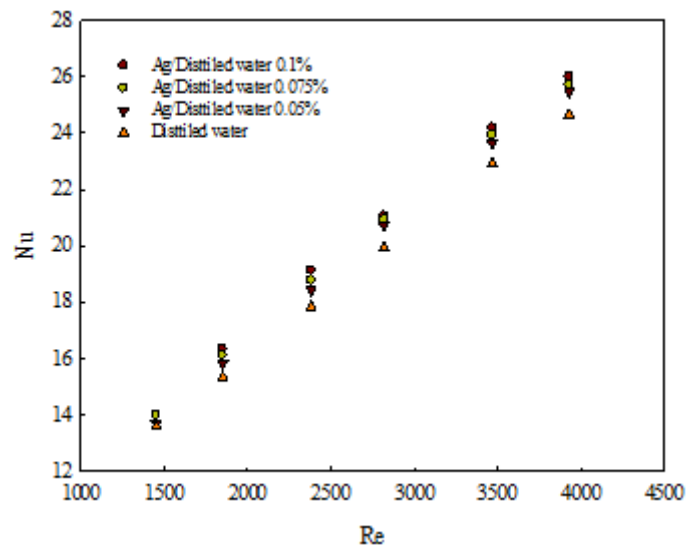


Fig. 13. Comparison of the Nusselt number with Reynolds number at different temperatures of base fluid and nanofluid, with volume fractions of 0.1%, 0.075% and 0.05%

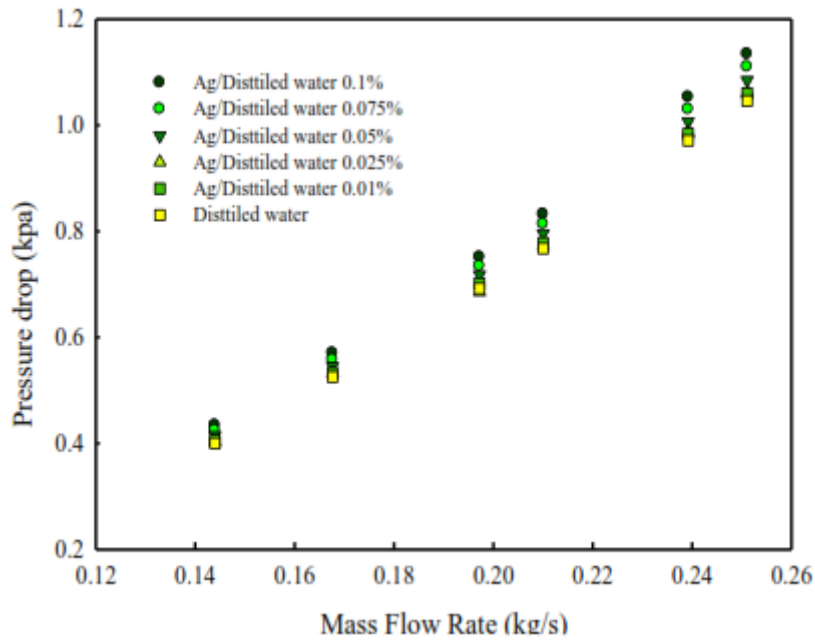


Fig. 14. Comparison of the pressure drop of distilled-water with silver nanofluid, with volume fractions of 0.01%, 0.025%, 0.05%, 0.075% and 0.1% at various temperatures and flow rates

Figure 16 shows the performance index of distilled-water/ silver nanofluid. The performance index is obtained from the overall heat transfer coefficient ratio of nanofluid to the overall heat transfer coefficient of distilled-water divided by the pressure drop ratio of nanofluid to the pressure drop of distilled-water. As inferred from Fig.16, the heat transfer enhancement is concomitant with increasing the pressure drop.

$$INDEX\ Number = \frac{(U_{nf}/U_{water})}{(\Delta p_{nf}/\Delta p_{water})} \quad (15)$$

If the index number is greater than 1, it is concluded that replacing the distilled-water/ silver nanofluid causes an increase in the heat transfer and if this ratio is equal to 1, it indicates the same performance of nanofluid and distilled water, but if the ratio is less than 1, it indicates that the performance of distilled-water in closed cycle cooling water system is more better than that of nanofluid.

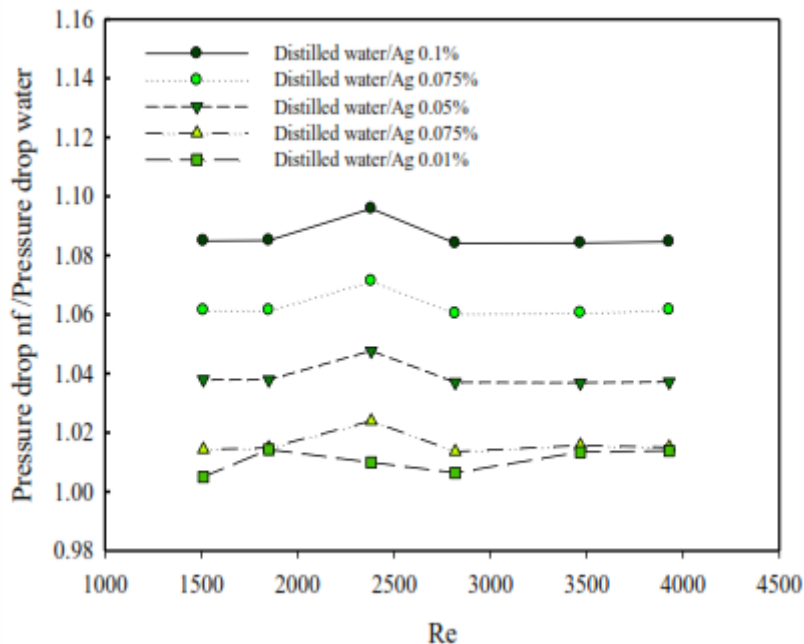


Fig. 15. The pressure drop ratio of distilled-water/silver nanofluid to distilled water

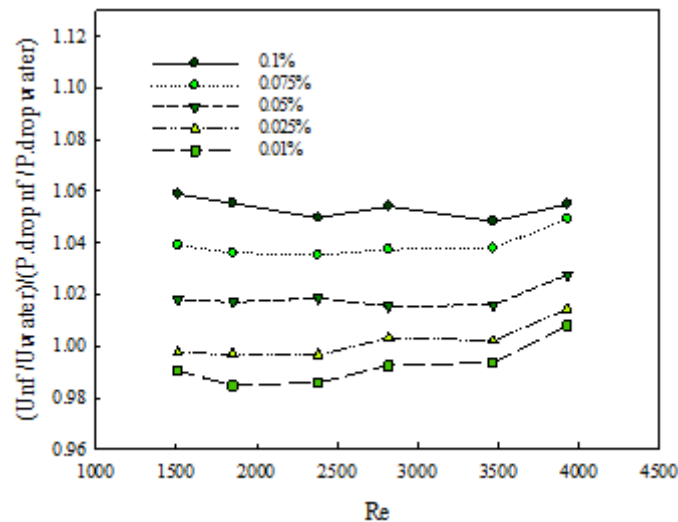


Fig. 16. Performance Index of distilled-water/silver nanofluid compared to pure distilled-water

## 7. Conclusion

In this study, the effect of distilled-water/silver nanofluid, with different volume fractions, on the heat transfer of closed cycle shell and tube heat exchanger at Isfahan power plant was studied experimentally. The results showed that the heat transfer properties of nanofluid were significantly improved with a rise in Reynolds number. In this experiment, an optimal volume fraction was obtained for the nanofluid in which the volume fraction of the heat transfer properties showed their maximum increase, where the optimal volume fraction in this experiment was 0.1%. In this study, the experiment was carried out up to 0.1%. However, the use of volume fraction >0.1% might be followed by the increased heat transfer, but the possibility of particle deposition was also increased and it was possible to find another optimal volume fraction with the highest heat transfer. The results of this study have been practically used in the coolers of boiler air preheaters in the third unit of Isfahan power plant.

## References

- [1] Farajollahi B., Etemad S.Gh., Hojjat M., Heat Transfer of Nanofluids in a Shell and Tube Heat Exchanger, *International Journal of Heat and Mass Transfer* (2010) 53: 12–1,.
- [2] Seifi Jamnani M., Hoseini S.M., Hashemabadi S.H., PeyGhambarzad S.M., Experimental Study of Al<sub>2</sub>O<sub>3</sub>/Water Nano-Fluid Flow Heat Transfer Through the Elliptical Tubes, *ICHEC13, Kermanshah- Iran* (2010).
- [3] Peyghambarzadeh SM., Hashemabadi SH., Seifi Jamnani M., Hoseini SM. Improving the Cooling Performance of Automobile Radiator with Al<sub>2</sub>O<sub>3</sub>/Water Nanofluid, *Applied Thermal Engineering* (2011) 31:1833–8.
- [4] Zamzamian A., Oskouie SN., Doosthoseini A., Joneidi A., Pazouki M., Experimental Investigation of Forced Convective Heat Transfer Coefficient in Nanofluids of Al<sub>2</sub>O<sub>3</sub>/EG and CuO/EG in a double pipe and plate heat Exchangers under Turbulent Flow, *Experimental Thermal and Fluid Science* (2011) 35(3):495–502.
- [5] Godson Asirvatham L., Raja B., Lal DM., Wongwises S., Convective Heat Transfer of Nanofluids with Correlations. *Particuology* (2011) 9:626–31.
- [6] Patel S., Patel V., Thakkar V., Experimental Investigation of Diameter Effect of Al<sub>2</sub>O<sub>3</sub> Nano Fluid on Shell and Tube Heat Exchanger in Laminar Flow Regime (2015) 2(5): Online ISSN: 2393-9877, Print ISSN: 2394-2444.
- [7] Dharun Arvind R., Heat Transfer Analysis Of Shell And Tube Heat Exchanger Using Aluminium Nitride / Water Nanofluid", *International Journal on Applications in Mechanical and Production Engineering* (2015) 1: 13-15.
- [8] Amani J., AbbasianArani A.A., Experimental Investigation of Diameter Effect on Heat Transfer Performance and Pressure Drop of TiO<sub>2</sub> Water Nano Fluid, *Experimental Thermal and Fluid Science* (2013) 44: 520-533.
- [9] Godson L., Deepak K., Enoch C., Heat Transfer Characteristics of Silver/Water Nano Fluids in a Shell and Tube Heat

- Exchanger, Archives of Civil and Mechanical Engineering (2014) 14: 489-496.
- [10] Afshoon Y., Fakhar A., Numerical Study of Improvement in Heat Transfer Coefficient of Cu-O Water Nanofluid in the Shell and Tube Heat Exchangers, Biosciences Biotechnology Research Asia (2014) 11(2): 739-747.
- [11] Baghmisheh Gh., Moradzadeh M., Hedayatzadeh S., Dorosti R., Industrial Heat Exchanger Design with ASPEN B-JAC (2007) 67-90.
- [12] Taylor J.R., An Introduction to Error Analysis, The Study of Uncertainties of Physical Measurements. University Science Books (1982).
- [13] Bork P.V., Grote H., Notz D., Regler M., Data Analysis Techniques in High Energy Physics Experiments. Cambridge University Press (1993).
- [14] Akhavan-Behabadi M.A., Mohseni S.G., Najafi H., Ramazanzadeh H. Heat Transfer and Pressure Drop Characteristics of Forced Convective evaporation in horizontal tubes with Coiled Wire Inserts, International Communications in Heat and Mass Transfer.